Submitted, accepted and published by

Fuel Processing Technology 176 (2018) 107-118

Assessment of the improvement of chemical looping combustion of coal by using a manganese ore as oxygen carrier

Alberto Abad, Pilar Gayán*, Teresa Mendiara, José A. Bueno, Francisco García-Labiano, Luis F. de Diego, Juan Adánez

Instituto de Carboquímica (ICB-CSIC), Miguel Luesma Castán, 4, Zaragoza, 50018, Spain

*Corresponding author: pgayan@icb.csic.es

Abstract

Finding suitable low-cost materials to be used as oxygen carrier in Chemical Looping Combustion (CLC) of coal is a key issue to achieve the CO_2 capture at low economic cost. Recently, a Mn-ore from Gabon has been identified as an alternative to the state of the art of oxygen carriers based on minerals or wastes with high iron content. This Mn-ore showed a high reactivity and a long particle lifetime during batch characterization to be considered as a suitable oxygen carrier. To evaluate the potential of this material in CLC, this work analyses the behaviour of the Mn-ore during continuous combustion of a bituminous coal in a 0.5 kW_{th} CLC unit. The CLC process was evaluated and the effect of the main operating variables -such as fluidizing medium, oxygen carrier circulation rate, temperature, and solids inventory in the fuel reactor- on the combustion efficiency and CO_2 capture was investigated. A direct relation between the char conversion rate and the CO_2 capture is given, being mainly affected by the mean residence time of solids and temperature in the fuel reactor. The use of a carbon separation system with separation efficiency above 90 % would be required to achieve CO_2 capture rates higher than 95 %. Total oxygen demand values as low as 4.5 % were found when optimal operating conditions were selected, mainly being related to oxygen carrier to fuel ration higher than $\phi > 3$. At these conditions, the Mn-ore material showed similar combustion efficiencies than other Fe-based low-cost materials previously tested, but with higher CO_2 capture rates.

Keywords: CO_2 capture; Chemical Looping Combustion; oxygen carrier; manganese ore; coal.

1. Introduction

New technologies are being investigated to reduce the CO_2 emissions to the atmosphere by fossil fuel combustion. Among them, Chemical Looping Combustion (CLC) has been highlighted as a promising one with low economic and energetic costs [1]. CLC is based in two reactor so-called fuel and air reactors with an oxygen carrier continuously circulating between them. In the fuel reactor, the fuel combustion happens using oxygen available in the oxygen carrier, usually being a metal oxide. In the air reactor, the oxygen carrier is regenerated by oxidation with air. In this way, air is not put in contact with the fuel, allowing the inherent CO_2 capture in the process, while the global chemical reaction and combustion enthalpy is the same than in normal combustion with air.

The development of the CLC with solid fuels has been mainly focused on the *in-situ* Gasification (*i*G-CLC) concept [2-4], where steam and/or recycled CO_2 are supplied to the fuel reactor as gasifying agents. A scheme of the CLC technology with solid fuels is shown in Fig.1. In-situ gasification of solid fuel takes place into the fuel reactor, as well as subsequent oxidation of the gasification products generated by gas-solid reactions with the oxygen carrier (M_xO_y). Thus, coal is oxidized to CO_2 and H_2O while the oxygen carrier is reduced. CO_2 in the product stream can be easily captured, once the water has been condensed. The reduced oxygen carrier (M_xO_{y-1}) is sent to the air reactor where it is oxidized with the oxygen in the air being ready to start a new redox cycle. In *i*G-CLC, the gasification is a slow step during the coal conversion, causing that some unconverted char could arrive at the air reactor, where it will be oxidized to CO_2, which would decrease the CO_2 capture efficiency of the process. A carbon separation step (e.g. carbon stripper reactor) between both fuel and air reactors is necessary to avoid this fact.

Complete combustion in case of gaseous fuels has been reached with the state of the art development of CLC [2]. However, complete combustion of coal to CO_2 and H_2O is not achieved so far in the *i*G-CLC process with solid fuels [3]. An oxygen polishing step would be required downstream the fuel reactor to oxidize unburnt products, which would require pure oxygen in order to maintain the advantage of the inherent CO_2 capture of the CLC process.

Some technological solutions have been proposed and evaluated in order to decrease the oxygen demand of the process [5]. In addition, the use of highly reactive oxygen carriers can help to decrease the oxygen demand of the *i*G-CLC process [6].

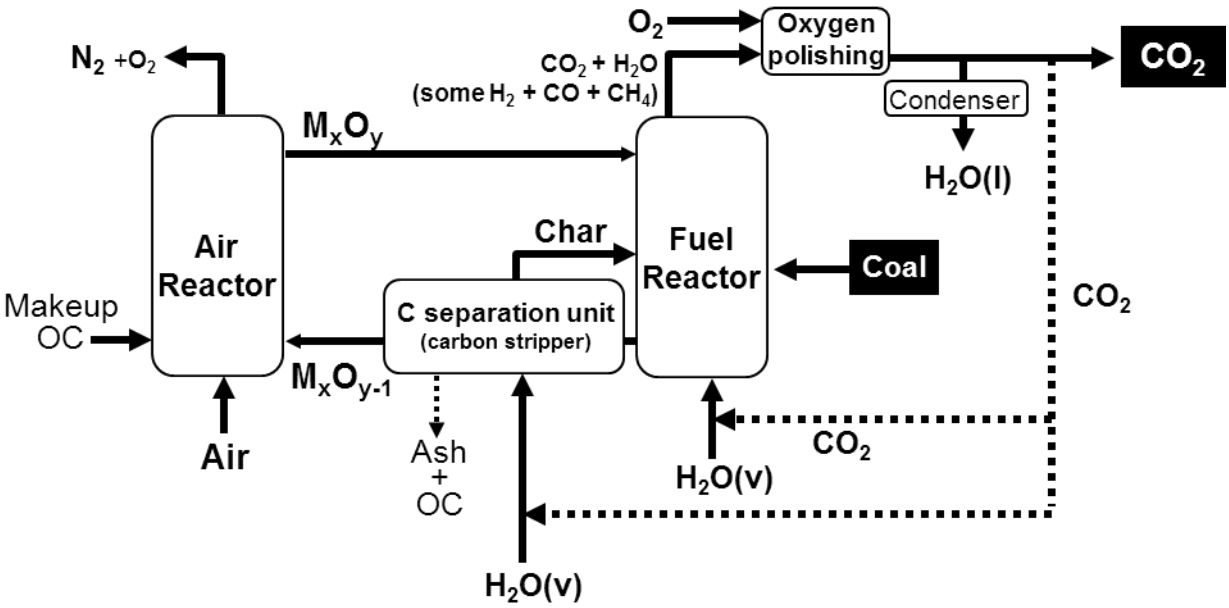

Fig. 1. Scheme of Chemical Looping Combustion with solid fuels.

Ash produced during solid fuel combustion should be drained to avoid their accumulation in the system. In this case, oxygen carrier particles will be also extracted in the drainage, which causes a loss of oxygen carrier. A make-up stream of oxygen carrier will be then necessary. Similarly to the development of oxygen carriers for gaseous fuels, some synthetic materials have been evaluated as oxygen carrier for CLC of coal [7]. However, the relatively lower price of natural minerals or waste materials compared to synthetic materials, makes that these low-cost oxygen carriers are attractive for the application in *i*G-CLC technology. Ilmenite and iron ores have been fully investigated so far [3], as well as waste materials with high iron or manganese content [8-10]. More recently, Mn-ores are being considered as an alternative for Fe-based materials due to its relatively high reactivity and its positive effect on the char conversion rate. Several Mn-ores from different origin -Norway in [9,10], Gabon in [9,11], Colombia in [12], in addition to S. Africa, Brazil, Slovakia, Egypt in [13,14] or China

and Ukraine in [15]- have been evaluated in thermogravimetric analysers or small fluidized bed facilities. Among them, Mn-ore from Brazil, Australia and Gabon have been considered as promising materials due to its high reactivity and good fluidization properties [11,16]. The char gasification rate in presence of these ores was faster than that observed in presence of other Fe-based materials such as ilmenite [17,18]. Alkali compounds (Na or K) transference from the Mn-ore to the char particles justified the improvement observed in char gasification [19]. The effect is similar to those observed with an iron material modified by K [20]. However, this effect was limited to a few redox cycles as Na or K was lost from the oxygen carrier material [18].

During 10 h of combustion with the Brazilian Mn-ore in a 10 kW_{th} CLC unit, improved CO_2 capture rates were attained compared to the use of ilmenite due to the enhancement of the char gasification rate [21]. The high attrition rate of this Brazilian ore forced to add new material continuously, thus incorporating fresh alkali elements, which are present in the Mn-ore, to the CLC unit. Similar conclusions were extracted from 18 h of combustion with ilmenite/Mn-ore mixtures and other Mn-ores in the 10 kW_{th} CLC unit [22,23], as well as with an Australian Mn-ore in a 100 kW_{th} CLC unit [24]. But the contrary was found during the combustion of biomass at the scale of 10 kW_{th} with braunite [25] and in a 2-4 MW_{th} unit with the Brazilian Mn-ore [26]. Nevertheless, the 2-4 MW_{th} unit is not optimized in terms of boiler temperature and oxygen carrier/fuel mixing for CLC operation, giving low combustion and CO_2 capture efficiency values.

Tested Mn-ores from Brazil and Australia showed high attrition rates, with estimated lifetime in the 100-400 h interval [11,23,24] which is much lower than those estimated for an iron ore [27]. Recently, a Mn-ore from Gabon has been investigated in TGA and small fluidized bed reactor [11,18]. This material showed good fluidization properties, neither agglomeration of particles nor de-fluidization was observed, (even if the oxygen carrier was highly reduced) with a relatively low attrition rate, with an estimated particle lifetime of 1000 h. In addition, the enhancement of the char gasification rate in the presence of this Mn-ore was observed even when alkali compounds were lost after several redox cycles at high temperature. Therefore,

this Mn-ore shows a great potential to be considered as oxygen carrier in CLC processes using solid fuels, but its behaviour during continuous coal combustion in a CLC unit must be still evaluated.

This work analyses the behaviour of the Mn ore from Gabon during 100 h in a 0.5 kW_{th} CLC unit for coal combustion. An extensive evaluation of the *i*G-CLC process was done, analysing the effect of main operating variables -such as temperature, oxygen carrier circulation rate, solids inventory and fluidizing medium- on the combustion efficiency and CO_2 capture. Results are further used to assess the potential of this Mn-ore to be used as oxygen carrier in comparison with the state of the art of Fe-based materials.

2. Experimental

2.1. Materials

A manganese ore from Gabon was used as oxygen carrier in the *i*G-CLC experiments. This material was supplied by Hidro Nitro Española S.A. Once received, it was crushed and sieved to the desired size (+100-300 μm). Then, particles of the manganese ore were thermally treated in air at 800 ºC for 2 h to ensure the complete oxidation prior its utilization. According to previous works [28-30], particles in the +100-300 μm interval show good fluidization properties to be used in the 0.5 kW_{th} CLC unit at ICB-CSIC, where the fuel reactor is fluidized in the bubbling regime. Table 1 shows the main properties of this oxygen carrier. After calcination in air, the Mn-ore was mainly constituted by Mn_2O_3 and Fe_2O_3. However, Mn_2O_3 was easily reduced to MnO under combustion conditions, which mostly could be oxidized to Mn_3O_4 [11]. Thus, for cycled particles the oxygen transport capacity, R_{OC}, was calculated considering the Mn_3O_4-MnO redox pair, together the oxygen available in iron oxide considering the Fe_2O_3-Fe_3O_4 redox pair [31].

Table 1. Characterization of the oxygen carrier.

Major active compounds[a]	68.2 wt% Mn_2O_3

	10.6 wt% Fe_2O_3
Oxygen transport capacity (wt%)[b]	7.3 (5.1)
Bulk density (kg/m^3)	2800
BET surface area (m^2/g)	12.3
Porosity (vol%)	38.7
Crushing strength (N)	1.8
AJI (%)	14.4

[a] Phase determination by XRD and quantified by TGA [11]

[b] Considering either Mn_2O_3/MnO or Mn_3O_4/MnO (in brackets) redox pair

A South African bituminous coal with medium volatile matter content was fed into the fuel reactor during the experimental campaign. The diameter of the coal particles was in the +200-300 μm interval, which was suitable to minimize the elutriation of fuel particles from the fuel reactor [28]. The proximate and ultimate analyses of the coal are shown in Table 2. The lower heating value (LHV) of the South African coal is 26430 kJ/kg.

Table 2. Main characteristics of the South African bituminous coal.

Proximate analysis (wt% raw matter)		Ultimate analysis (wt% raw matter)	
Moisture	4.2	C	69.3
Volatile matter	25.5	H	3.5
Fixed carbon	56.0	N	2.0
Ash	14.3	S	1.0
		O[a]	5.7

[a] Oxygen by difference

2.2. Experimental set up

The combustion experiments were performed at the continuous ICB-CSIC-s1 unit of 0.5 kW_{th}; see Fig. 2. The CLC facility consist of two interconnecting bubbling fluidized bed

reactors as fuel and air reactors connected by a loop seal. The heating of the fuel and air reactor by electric furnaces was required to support the operation at high temperature due to the high thermal losses of the unit associated to its small size. The fuel reactor is 50 mm ID and 200 mm bed height. The coal is fed by using a screw feeder just above the fuel reactor distributor plate, and here it is gasified. The screw feeder has two steps [28]: the first one regulates the coal feeding rate; the second one rotates at high speed to ensure a rapid entry of coal to the bed, thus minimizing the pyrolysis inside the screw feeder. This system guarantees a constant and stable feeding of the solid fuel.

A total flow of 120 L/h (STP) of steam/CO_2 mixtures is used as fluidizing and gasifying agent. Then, gasification products are oxidized by reacting with the oxygen carrier. The molar ratio of gasifying agent to carbon in fuel was above 1.7, which would allow a proper operation of a CLC unit [32]. The oxygen carrier moves to the air reactor through the loop seal, which is fluidized by 120 L/h (STP) N_2 in order to avoid the mixing of air and fuel reactor gases. The oxygen carrier is re-oxidized in the air reactor (80 mm ID and 100 mm bed height), which is fluidized by 2000 L/h (STP) air. The upper part of the air reactor was designed as a narrow and long riser (30 mm ID and 1.2 m height) to guarantee an adequate flow of solids from the air reactor to the fuel reactor. Then, the oxygen carrier is separated from the exhaust air by a high-efficiency cyclone. The particles are accumulated in a solid reservoir which avoids the mixing of gases in the riser with gases in the fuel reactor. The solids flow between both reactors was regulated by a conical solid valve, which connect the solids reservoir to the fuel reactor. Thus, loop of solids circulation is closed. In addition, the solids circulation rate can be measured with a solids diverter valve.

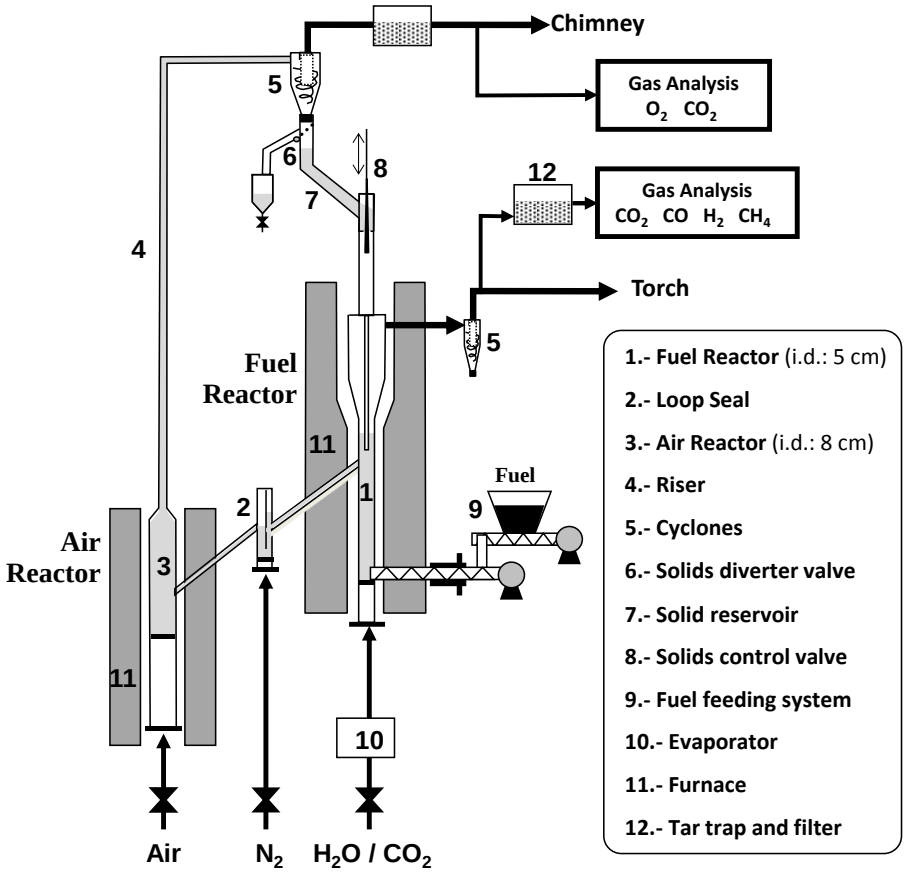

Fig. 2. Experimental 0.5 kW_{th} CLC unit ICB-CSIC-s1 for solid fuel combustion.

The concentration of the main gases in the outlet streams of the fuel reactor (CO_2, CO, H_2, CH_4 and O_2) and air reactor (O_2, CO_2 and CO) was measured after gas drying. CO_2, CO and CH_4 concentration values were measured by a non-dispersive infrared (NDIR) analyzer (Siemens Ultramat 23); H_2 concentration was measured by a thermal conductivity detector (Maihak S710/THERMOR); and O_2 concentration was obtained using a paramagnetic analyzer (Siemens 23/Oxymat 6). The temperature of fuel and air reactors was registered by using thermocouples inside the beds. Also, the pressure drop of every reactor was measured with pressure sensors.

2.3. Experimental procedure

A total amount of 3 kg Mn ore was introduced in the plant. No addition of new material was done during the entire experimental campaign. Every day, the CLC unit was heated to the

desired operating temperature in air, assuring a complete oxidation of the oxygen carrier before the experimental tests started. Then, the steam flow to the fuel reactor and air flow to the air reactor were fixed to achieve a gas velocity of 0.08 m/s and 0.5 m/s, respectively. Following, the desired solids circulation rate was fixed with the help of the conical solids control valve. The solids circulation rate was measured before and after each test to check if it was maintained constant throughout the experiment. Once the desired operating conditions were achieved, coal fed started. The coal feeding rate was maintained roughly constant to 55 g/h during all the tests, corresponding to 0.4 kW_{th}. In every test, steady state was maintained at least for one hour.

Different combustion tests were performed varying several operating conditions; see Table 3. The fuel reactor temperature was varied from 890 °C to 964 °C. The temperature in the air reactor was maintained at around 950°C. The amount of solids in the fuel reactor was calculated by determining the pressure drop. Thus, solids in the fuel reactor were in the 0.46-0.60 interval, which corresponded to a specific solids inventory, m_{FR}^{*} , in the 965-1561 kg/MW_{th} interval. Also, the solids circulation flow rate, $\dot{m}_{OC}$, was varied between 2.6 and 13.3 kg/h to analyse the effect of the oxygen carrier to fuel ratio (ϕ parameter) on the performance of the system in a wide interval (ϕ=1.1-5.7). The ϕ parameter is defined as the amount of the oxygen available in the fuel reactor, which is transported by the oxygen carrier flow from the air reactor, respect the stoichiometric oxygen demanded by the coal fed, calculated by:

$$\phi = \frac{R_{OC} \cdot \dot{m}_{OC}}{\dot{m}_{coal} \cdot \Omega_{coal}} \quad (1)$$

$\dot{m}_{OC}$ being the oxygen carrier circulation flow rate, $\dot{m}_{coal}$ the coal feeding rate, and Ω_{coal} the stoichiometric mass of oxygen required to burn 1 kg of coal (Ω_{coal} = 2.1 kg O/kg coal).

Most of experiments were carried out using steam as fluidizing and gasifying medium. But also the effect of the fluidizing medium was studied by doing some tests with steam/CO_2 mixtures. In these cases, the total flow of gas to the fuel reactor was maintained constant.

Table 3. Main operating conditions and evaluating parameters for the experimental tests performed burning bituminous coal with Mn-ore.

Test	H_2O	T_{FR}	Power	m_{FR}	m^*_{FR}	$\dot{m}_{OC}$	ϕ	X_{sf}	X_{char}	η_{CC}	$X_{char,FR}$	Ω_T	$\eta_{comb,FR}$
	vol%	ºC	kW_{th}	kg	kg/MW_{th}	kg/h	-	%	%	%	%	%	%
T1	100	930	0.39	0.48	1240	2.6	1.1	91.2	89.1	83.1	78.5	12.6	83.9
T2	100	932	0.39	0.48	1236	5.2	2.3	83.5	79.5	71.4	62.8	7.2	88.9
T3	100	932	0.40	0.49	1230	8.4	3.5	83.9	80.1	62.8	51.8	5.0	92.0
T4	100	931	0.40	0.49	1231	9.6	4.0	85.7	82.3	59.3	47.5	4.3	92.5
T5	100	927	0.40	0.48	1206	13.3	5.6	88.3	85.5	54.9	42.3	4.6	91.7
T6	100	936	0.37	0.54	1455	8.5	3.9	92.0	90.1	60.4	50.0	4.5	92.0
T7	100	928	0.38	0.54	1424	11.9	5.3	88.7	86.0	56.8	44.9	4.6	91.9
T8	100	932	0.37	0.54	1463	12.4	5.7	93.3	91.8	56.7	45.5	4.4	92.5
T9	100	927	0.40	0.48	1206	13.3	5.6	88.3	85.5	54.9	42.3	4.6	91.7
T10	100	932	0.37	0.54	1463	12.4	5.7	93.3	91.8	56.7	45.5	4.4	92.5
T11	100	928	0.38	0.59	1561	11.6	5.1	90.4	88.1	59.2	48.2	4.7	92.0
T12	100	929	0.60	0.58	965	8.6	2.4	90.6	88.4	63.4	53.5	5.4	91.4
T13	100	932	0.39	0.48	1236	5.2	2.3	83.5	79.5	71.4	62.8	7.2	88.9
T14	100	939	0.39	0.52	1331	6.1	2.6	90.2	87.8	70.8	62.9	5.6	91.7
T15	100	895	0.37	0.50	1360	3.7	1.6	90.4	88.1	59.1	48.1	8.0	86.0
T16	100	909	0.37	0.49	1314	4.8	2.2	90.3	88.0	63.2	53.2	8.0	86.0
T17	100	910	0.37	0.48	1307	3.7	1.7	85.4	81.9	64.0	53.5	8.3	86.3
T18	100	917	0.37	0.54	1466	4.1	1.9	88.0	85.1	68.8	60.1	8.6	86.9
T19	100	917	0.37	0.50	1352	4.8	2.2	92.2	90.3	64.2	54.8	8.9	86.1
T20	100	932	0.39	0.48	1236	5.2	2.3	83.5	79.5	71.4	62.8	7.2	88.9
T21	100	947	0.38	0.51	1337	5.3	2.3	90.6	88.3	76.0	69.5	8.4	88.4
T22	100	964	0.39	0.48	1223	3.7	1.6	90.2	87.9	82.9	78.3	8.0	89.7
T23	100	890	0.37	0.50	1354	6.7	3.0	90.3	88.0	50.3	36.9	6.6	87.2
T24	100	895	0.37	0.49	1332	6.2	2.8	90.2	87.9	53.4	40.8	8.2	85.0
T25	100	902	0.37	0.48	1303	6.8	3.1	89.5	87.0	55.1	42.8	7.0	87.3
T26	100	920	0.37	0.52	1400	6.9	3.1	93.4	91.2	59.6	49.1	7.4	87.9
T27	100	926	0.39	0.51	1315	6.2	2.7	90.4	88.1	63.6	53.8	6.3	90.0
T28	100	935	0.38	0.50	1323	6.5	2.9	90.7	88.5	66.5	57.5	7.1	89.1
T29	100	935	0.38	0.50	1322	7.9	3.5	93.6	92.0	65.7	56.8	8.0	87.9

T30	100	939	0.39	0.52	1331	6.1	2.6	90.2	87.8	70.8	62.9	5.6	91.7
T31	100	941	0.38	0.52	1380	6.3	2.8	92.2	90.3	68.3	60.0	7.8	88.4
T32	100	944	0.38	0.51	1330	6.3	2.8	91.0	88.8	68.8	60.4	8.1	88.0
T33	100	946	0.39	0.44	1128	7.0	3.0	89.6	87.2	68.0	59.3	7.7	88.3
T34	100	945	0.38	0.50	1323	6.45	2.9	90.7	88.5	65.9	56.6	7.0	89.1
T35	67	940	0.39	0.50	1298	6.88	3.0	98.5	99.2	62.4	54.4	7.0	90.2
T36	50	943	0.39	0.50	1341	5.50	2.4	90.6	88.4	62.0	52.2	6.6	89.6
T37	0	939	0.39	0.50	1269	6.40	2.8	91.0	88.8	47.5	35.4	5.9	89.2

2.4. Data evaluation

The coal combustion throughput in the 0.5 kW_{th} CLC unit with Mn ore was evaluated by using three main features [3]: the fuel conversion, the CO_2 capture, and the combustion efficiency. These parameters were calculated after the calculation of the flow of every compound in the gaseous stream both from the air and fuel reactors, which was calculated by knowing the N2 flow that is introduced in the fuel-reactor coming from the loop seal. A detailed description of the used methodology is shown elsewhere [28].

2.4.1. Fuel conversion

The fuel conversion evaluates the fraction of coal converted in the CLC unit, i.e. both the fuel and air reactors. A carbon balance is considered to analyse the amount of coal converted. Thus, the solid fuel conversion, X_{sf}, is the fraction of carbon in coal being converted in the CLC unit.

$$X_{sf} = \frac{\left[F_{CO_2} + F_{CO} + F_{CH_4}\right]_{outFR} + \left[F_{CO_2}\right]_{outAR} - \left[F_{CO_2}\right]_{inFR}}{\dot{m}_{coal} x_C} M_C \quad (2)$$

The amount of carbon detected in the gaseous streams is lower than the carbon in the fed coal. In some selected experiments higher hydrocarbons (C2-C5) were analysed by gas chromatography, and the tar amount present in fuel reactor product gases was determined following the tar protocol [33]. These analyses showed that there was neither C2-C5 nor tars in the fuel reactor outlet flow. This result agrees to the previously obtained with Fe-based

oxygen carriers in this CLC unit [28-30]. Therefore, unseen carbon was assumed to be present in unconverted char particles elutriated from the fuel reactor. Thus, an additional parameter, the char conversion in the CLC unit (X_{char}), can be used to evaluate the fraction of fixed carbon being elutriated, and therefore non-converted in the CLC unit.

$$X_{char} = \frac{\left[F_{CO_2} + F_{CO} + F_{CH_4}\right]_{outFR} + \left[F_{CO_2}\right]_{outAR} - [F_{CO_2}]_{inFR} - [F_C]_{vol}}{\dot{m}_{coal} x_{C,fix}} M_C \quad (3)$$

$[F_C]_{vol}$ being the flow of carbon in the gases coming from volatile matter.

The flow of carbon elutriated is calculated by the following carbon balance:

$$F_{C,elut} = \dot{m}_{coal} \frac{x_C}{M_C} - \left\{\left[F_{CO_2} + F_{CO} + F_{CH_4}\right]_{outFR} + \left[F_{CO_2}\right]_{outAR} - [F_{CO_2}]_{inFR}\right\} \quad (4)$$

2.4.2. CO_2 capture

The CO_2 capture efficiency (η_{CC}) is defined as the fraction of the carbon in the gaseous streams from the CLC unit which is actually exiting from the fuel reactor.

$$\eta_{CC} = \frac{\left[F_{CO_2} + F_{CO} + F_{CH_4}\right]_{outFR} - [F_{CO_2}]_{inFR}}{\left[F_{CO_2} + F_{CO} + F_{CH_4}\right]_{outFR} + \left[F_{CO_2}\right]_{outAR} - [F_{CO_2}]_{inFR}} \quad (5)$$

It can be considered that coal is quickly devolatilized in the fuel reactor, and all carbon present in volatile matter is actually exiting from the fuel reactor as different compounds, e.g. CO, CH_4 or CO_2. Therefore, the CO_2 capture is directly affected by the conversion of char in the fuel reactor, $X_{char,FR}$, which is defined as the fraction of fixed carbon gasified in the fuel reactor with regard to the fixed carbon converted in the whole CLC unit.

$$X_{char,FR} = \frac{\left[F_{CO_2} + F_{CO} + F_{CH_4}\right]_{outFR} - [F_{CO_2}]_{inFR} - [F_C]_{vol}}{\left[F_{CO_2} + F_{CO} + F_{CH_4}\right]_{outFR} + \left[F_{CO_2}\right]_{outAR} - [F_{CO_2}]_{inFR} - [F_C]_{vol}} \quad (6)$$

Note that char neither gasified nor elutriated in the fuel reactor will be eventually burned in the air reactor, given non-captured CO_2.

2.4.3. Combustion efficiency

The combustion efficiency is evaluated by calculating the amount of oxygen required to fully convert to CO_2 and H_2O the gases exiting the fuel reactor. Thus, the total oxygen demand,

Ω_T, represents the fraction of oxygen required to fully oxidize the unconverted gases exiting the fuel reactor compared to the oxygen needed for complete combustion of the coal fed.

$$\Omega_T = \frac{\left[F_{H_2} + F_{CO} + 4F_{CH_4}\right]_{outFR}}{\dot{m}_{coal}\Omega_{coal}} M_O \quad (7)$$

Another parameter often used to evaluate the combustion efficiency burning a solid fuel in a CLC unit is the oxygen demand in the fuel reactor, Ω_{FR}, which is related to the combustion efficiency in the fuel reactor, $\eta_{comb,FR}$.

$$\eta_{comb,FR} = 1 - \Omega_{FR} = 1 - \frac{\left[F_{H_2} + F_{CO} + 4F_{CH_4}\right]_{outFR}}{\dot{m}_{coal}\Omega_{coal} - 2M_O\left\{[F_{CO_2}]_{outAR} + F_{C,elut}\right\}} M_O \quad (8)$$

In this case, the oxygen required to combust the coal being actually converted in the fuel reactor is considered to evaluate the combustion efficiency; see denominator in Eq. (8).

3. Results

A total of 100 hours of continuous operation feeding fuel and 160 hours of continuous fluidization were accumulated during this experimental campaign. The Mn ore showed initially the capability to release gaseous oxygen at high temperatures, i.e. showed an initial oxygen uncoupling capability [34]. Thus, during the loading of the CLC unit with the Mn ore, which was done at temperatures above 900 ºC, Mn_2O_3 initially present in the calcined Mn ore (see Table 1) was decomposed to Mn_3O_4. Therefore, the experimental campaign was carried out at conditions at which Mn_3O_4 was reduced to MnO in the fuel reactor, while MnO was mostly oxidized to Mn_3O_4 in the air reactor. In addition, the bed material was mainly oxygen carrier during the entire experimental campaign, as ash particles were not recovered by the cyclone and they were not accumulated in the system.

Tests carried out were useful to evaluate the effect of different operating conditions, such as temperature, solids circulation rate, solids inventory and fluidizing agent, on the performance of the Mn ore burning coal by CLC. The average conversion of the solid fuel in the CLC unit was $X_{sf} \approx 90\%$, being elutriated approximately 10 % of the carbon in coal. Now, the effect of operating conditions on the CO_2 capture and combustion efficiency is presented. Later, some

projections are estimated to evaluate the process with a complete conversion of the fuel in the CLC unit.

3.1. CO_2 capture

The CO_2 capture efficiency, calculated by Eq. (5) was evaluated by changing the operating conditions in the 0.5 kW_{th} CLC unit. In all cases, some CO_2 was found to be in the air reactor exhaust gases. Considering that only carbon from the fuel reactor is captured by a CLC unit, the CO_2 capture efficiency was lower than 100 % due to char was not fully converted in the fuel reactor. Unconverted char is transferred to the air reactor together the oxygen carrier stream, and here it was burnt by air to non-captured CO_2. The fraction of unconverted char bypassed to the air reactor depended on the operating conditions.

It is well known that the CO_2 capture is highly affected by the residence time of solids and temperature in the fuel reactor [3,35,36]. First, the effect of the solids circulation rate was evaluated by considering the oxygen carrier to fuel ratio, ϕ; see Eq. (1). Note that a value of ϕ = 1 means that the stoichiometric oxygen required to burn the coal fed is supplied by the oxygen carrier. Fig. 3(a) shows the effect of the ϕ parameter on the CO_2 capture. Two series were obtained depending on the specific solids inventory in the fuel reactor, namely 1230 and 1450 kg/MW_{th}. The CO_2 capture is decreasing as ϕ increases due to the decrease in the residence time of solids in the fuel reactor. Thus, the char conversion also decreased, as it is shown in Fig. 3(a), which directly affects to the CO_2 capture. A direct relationship between the char conversion in the fuel reactor, $X_{char,FR}$, and the residence time of solids in the fuel reactor is shown in Fig. 3(b).

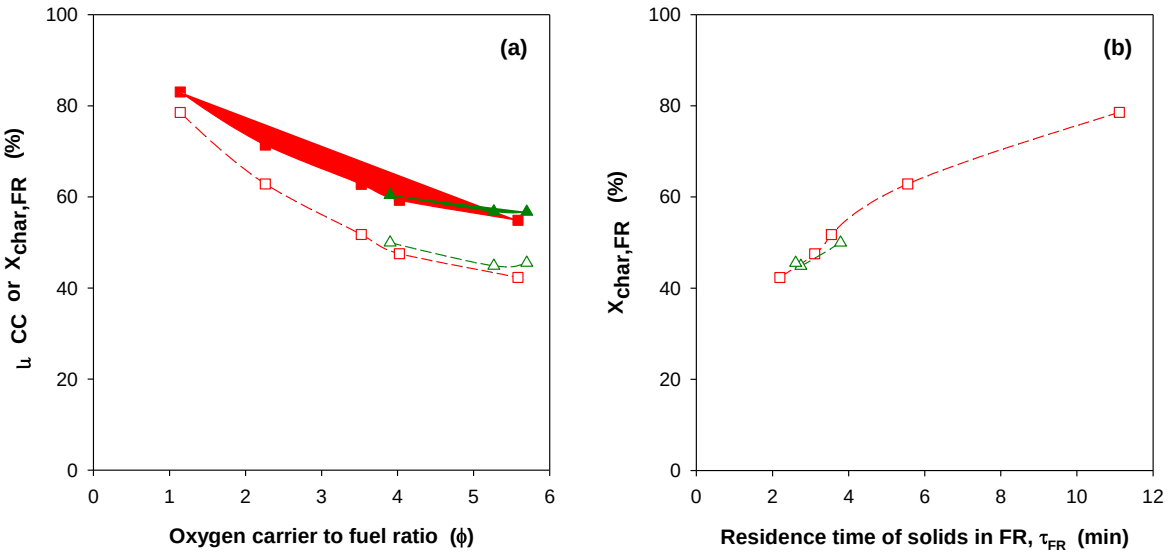

Fig. 3. (a) Effect of the oxygen carrier to fuel ratio, ϕ, on the CO_2 capture efficiency (η_{CC}: ■,▲) and char conversion in the fuel reactor ($X_{char,FR}$: □,Δ); and (b) influence of the residence time of solids in the fuel reactor, τ_{FR}, on $X_{char,FR}$. Specific solids inventory: T1-T5 (■□ with m^*_{FR} =1230 kg/MW) and T6-T8 (▲Δ with m^*_{FR} =1450 kg/MW). T_{FR} = 930 ºC.

In Figs. 3 a low effect of the specific solids inventory in the fuel reactor is observed due to the small variation in the mean solids residence time. In order to better evaluate the effect of the specific solids inventory, two more series were performed changing the amount of solids in the fuel reactor. In each series, the ϕ parameter was maintained roughly constant. Fig. 4(a) shows that the CO_2 capture efficiency and the char conversion in the fuel reactor increased with the specific solids inventory in the fuel reactor. This fact was related to the increase of the residence time of solids in the fuel reactor as the amount of solids was higher. In addition, both η_{CC} and $X_{char,FR}$ were higher in the series with a lower ϕ parameter, i.e. with lower solids circulation rate. This effect is clearly shown in Fig. 4(b), where $X_{char,FR}$ monotonically increase with the mean residence time of solids in the fuel reactor. As can be seen in Fig 4(b), the results obtained with the two series (ϕ values of 2.5 and 5.5) are in the same trend, therefore the residence time distribution is the main variable affecting the char conversion.

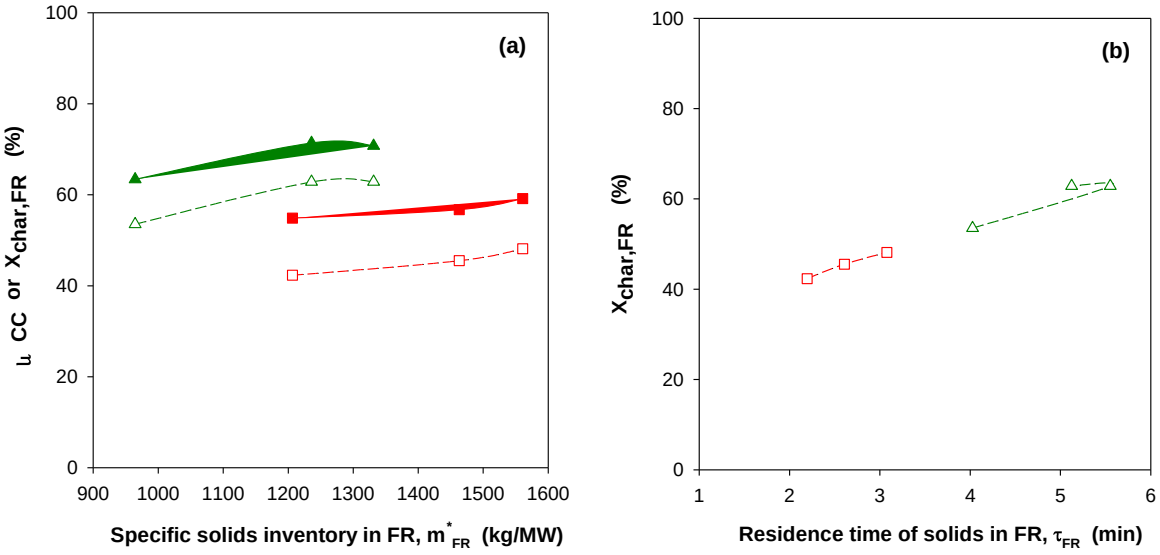

Fig. 4. (a) Effect of the specific solids inventory in the fuel reactor, m^{*}_{FR}, on the CO_2 capture efficiency (η_{CC}: ■,▲) and char conversion in the fuel reactor ($X_{char,FR}$: □,Δ); and (b) influence of the residence time of solids in the fuel reactor, τ_{FR}, on $X_{char,FR}$. Oxygen carrier to fuel ratio: T9-T11 (■□ with $\phi \approx 5.5$) and T12-T14 (▲Δ with $\phi \approx 2.5$). T_{FR} = 930 ºC.

The effect of the fuel reactor temperature on the CO_2 capture was also investigated in two different series involving tests T15-T22 ($\phi \approx 2$ and $\tau_{FR} \approx 7$ min) and T23-T33 ($\phi \approx 3$ and $\tau_{FR} \approx 4.5$ min); see Fig. 5(a). It can be seen the beneficial effect of the fuel reactor temperature on the CO_2 capture efficiency due to the increase of the char conversion in the fuel reactor. In addition, the CO_2 capture was higher with the lowest oxygen carrier to fuel ratio of $\phi = 2$ due to the lower solids circulation rate. This fact agrees to those previously observed in Fig. 3, where it was concluded that a lower solids circulation rate improves the char conversion in the fuel reactor because the higher residence time of solids in the fuel reactor.

From the collected experimental data, the rate of char gasification, ($-r_C$) was calculated considering the mean residence time of solids in the fuel reactor, τ_{FR} [30].

$$\left(-r_C\right) = \frac{1}{\tau_{FR}} \frac{X_{char,FR}}{1 - X_{char,FR}} \tag{9}$$

Fig. 5(b) shows the values of the calculated $X_{char,FR}$ as a function of temperature in the form of Arrhenius plot, i.e. $\ln(X_{char,FR})$ vs. $1/T_{FR}$. The char gasification rate increases with the

temperature regardless the oxygen carrier to fuel ratio used. This fact suggests that the fuel reactor temperature determines the char gasification rate, and the char conversion in the fuel reactor is additionally affected by the solids residence time, as it was observed when either solids circulation rate or the solids inventory in the fuel reactor was modified; see Figs. 3 and 4. The apparent activation energy for the char gasification was calculated assuming an Arrhenius type dependence.

$$\left(-r_C\right) = k_{0,app} e^{-\frac{E_a}{R_g T_{FR}}} \tag{10}$$

From the linearization shown in Fig. 5(b), values of $k_{0,app}$ = 6.5·10^7 s^{-1} and E_a = 234.2 kJ/mol were obtained. These values will be useful further to extrapolate results at higher temperatures.

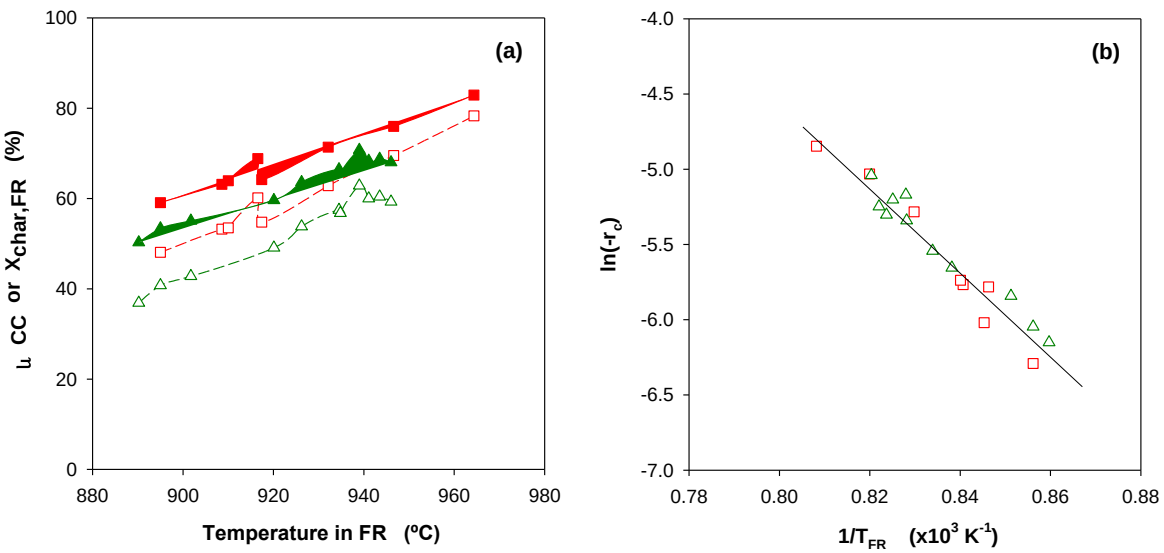

Fig. 5. (a) Effect of the fuel reactor temperature on the CO_2 capture efficiency (η_{CC}: ■,▲) and char conversion in the fuel reactor ($X_{char,FR}$: □,Δ); and (b) Arrhenius plot of the char gasification rate, ($-r_C$). Oxygen carrier to fuel ratio: T15-T22 (■□ with $\phi \approx 2$) and T23-T33 (▲Δ with $\phi \approx 3$). m^*_{FR} ≈ 1300 kg/MW$_{th}$.

Additionally, the effect of using steam or CO_2 as the fluidizing medium on the CO_2 capture was investigated. For it, different steam/CO_2 mixtures ranging from pure steam to pure CO_2

were used in tests T34-T37. The CO_2 capture was decreased as the fraction of CO_2 was higher in the fluidizing medium; see Fig. 6. This fact is related to the lower gasification rate of char with CO_2 compared to steam. Thus, the char conversion in the fuel reactor was lower as higher was the CO_2 concentration. However, a lineal decrease of η_{CC} or $X_{char,FR}$ with the CO_2 concentration is not observed. This fact suggests that the use of limited fractions of CO_2 can be allowed in the fluidizing medium without inducing a dramatic detriment of the CO_2 capture efficiency. The use of steam/CO_2 mixtures can benefit the CLC economy because that decreases the steam duty of the process, so decreasing the energy requirements in the steam generation. The required CO_2 can be obtained from the same CLC process by recirculating a fraction of exhaust gases from the fuel reactor; see Fig. 1.

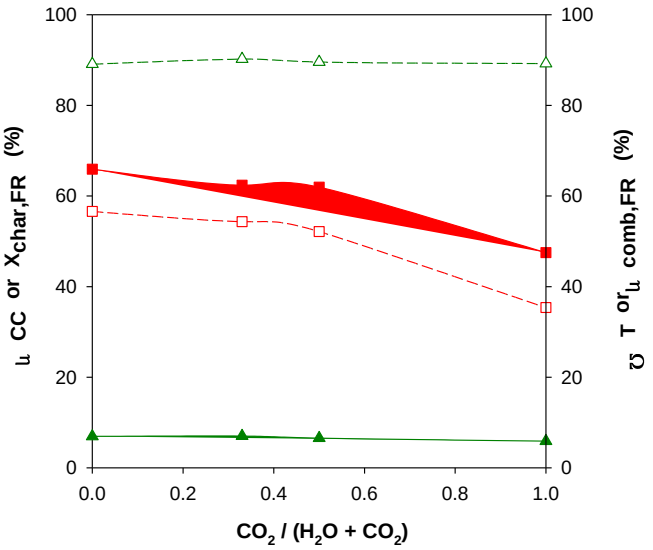

Fig. 6. Effect of the CO_2 concentration in the fluidizing medium on the CO_2 capture efficiency (η_{CC}: ■), char conversion in the fuel reactor ($X_{char,FR}$: □), total oxygen demand (Ω_T: ▲) and combustion efficiency in the fuel reactor ($\eta_{comb,FR}$: Δ). T_{FR} ≈ 940 ºC; ϕ ≈ 2.8. m^*_{FR} ≈ 1300 kg/MW_{th}.

3.2. Combustion efficiency

In all the tests performed in this study some unconverted compounds were present at the fuel reactor outlet, mainly H_2, CO and CH_4. In order to evaluate the amount of unconverted

gases in the fuel reactor both the total oxygen demand, Ω_T, and the combustion efficiency in the fuel reactor, $\eta_{comb,FR}$, were calculated; see Eqs. (7) and (8). Figs 7(a) and 7(b) shows the effect of the ϕ parameter and the solids inventory in the fuel reactor, respectively, on Ω_T and $\eta_{comb,FR}$.

On the one hand, both Ω_T and $\eta_{comb,FR}$. were affected at low ϕ values, i.e. low solids circulation flow rates. Thus, the total oxygen demand decreased as ϕ increased from 1 to 3. However, a further increase in the ϕ value did not showed a relevant effect on the total oxygen demand, reaching minimum values of Ω_T = 4-5% for ϕ > 3. Similar effect was observed for $\eta_{comb,FR}$. This effect is related to the variation of the mean reactivity of the oxygen carrier with the ϕ parameter. In general, the mean reactivity increases as the solids circulation rate increases, corresponding to higher ϕ values [37]. However, this increase is of lower relevance for ϕ > 3, which means that further increase of the solids circulation rate above $\phi \approx 3$ barely could affect to the combustion efficiency or oxygen demand.

On the other hand, the solids inventory in the fuel reactor barely affected to the total oxygen demand or combustion efficiency in the fuel reactor. Here it can be speculated that most of the unconverted gases comes from volatile matter, as gasification products are usually highly converted in the 0.5 kW_{th} CLC unit, characterized by a fuel reactor fluidized in the bubbling regime [28]. At this condition, a low contact efficiency between volatile matter, mainly emitted in a volatile plume, and oxygen carrier particles can be expected [3] and, as a result, an increase in the solids inventory did not have a relevant effect on the combustion efficiency of volatile matter.

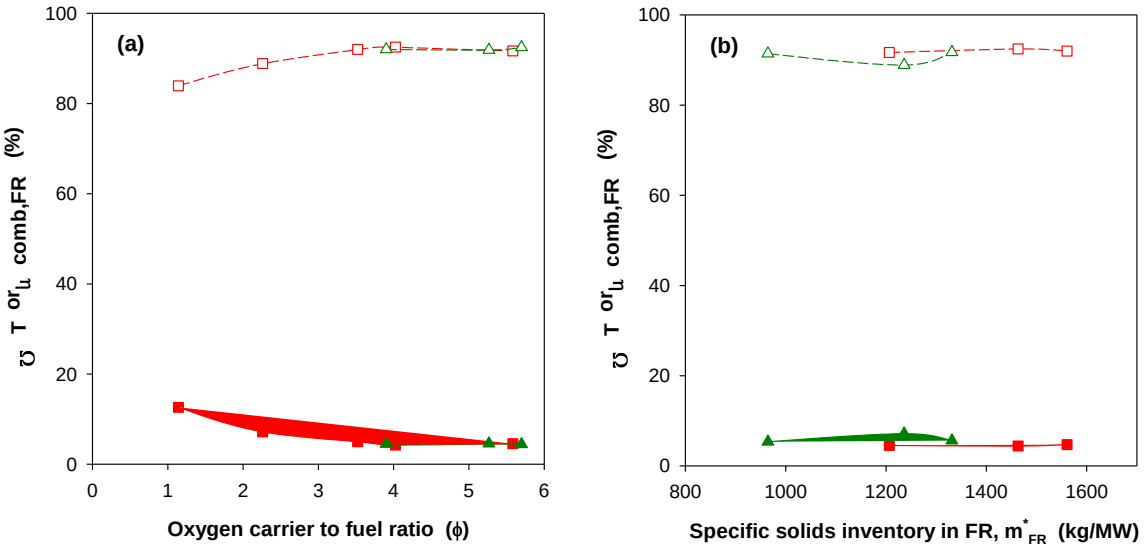

Fig. 7. Total oxygen demand (Ω_T: ■,▲) and combustion efficiency in the fuel reactor ($\eta_{comb,FR}$: □,Δ) as a function of (a) the oxygen carrier to fuel ratio, ϕ (tests T1-T5: ■□ with m^*_{FR} =1230 kg/MW and T6-T8 ▲Δ with m^*_{FR} =1450 kg/MW; and (b) the specific solids inventory in the fuel reactor, m^*_{FR} (tests T9-T11: ■□ with ϕ ≈ 5.5 and T12-T14: ▲Δ with ϕ ≈ 2.5). T_{FR} = 930 ºC.

In addition, the combustion efficiency in the fuel reactor, $\eta_{comb,FR}$, showed a slight increase with the fuel reactor temperature; see Fig. 8. However, the total oxygen demand, Ω_T, was barely affected by the temperature. This different behaviour was due to the way which Ω_T and $\eta_{comb,FR}$ are defined. Thus, a roughly constant Ω_T value means that the amount of unconverted products did not vary with temperature as the coal feeding rate was approximately the same; see Eq. (7). Taking this finding in mind, an increase of $\eta_{comb,FR}$ with temperature is related to a higher amount of coal being converted in the fuel reactor, i.e. denominator in Eq. (8). As a conclusion, the amount of unconverted gases is independent of the char fraction converted in the fuel reactor. As it was explained in the previous paragraph, likely gasification products are highly converted in the unit, while volatile matter are less converted due to a poor contact between volatiles and oxygen carrier particles. Therefore, unburnt products in the unit came from volatile. A deeper analysis on this assumption will be presented in the next section.

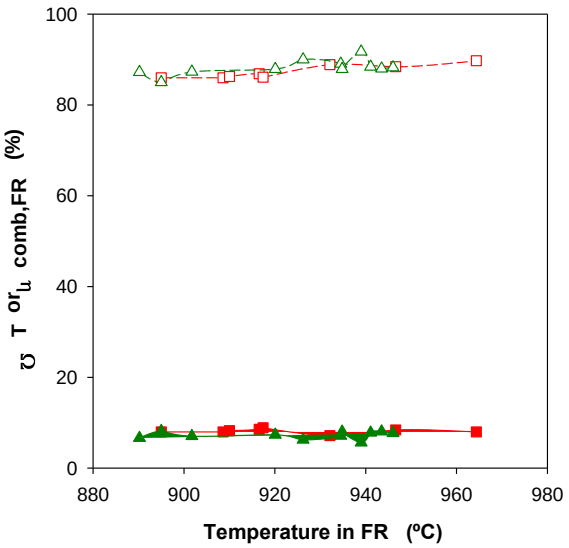

Fig. 8. Effect of the fuel reactor temperature on the total oxygen demand (Ω_T: ■,▲) and combustion efficiency in the fuel reactor ($\eta_{comb,FR}$: □,Δ). Tests T15-T22 (■□ with $\phi \approx 2$) and tests T23-T33 (▲Δ with $\phi \approx 3$). $m^*_{FR} \approx 1300$ kg/MW$_{th}$.

Finally, the combustion efficiency of the CLC process was not affected by the gasification medium, as both Ω_T and $\eta_{comb,FR}$ values were unaffected by the use of steam, CO_2 or steam/CO_2 mixtures as fluidizing gas; see Fig. 6.

4. Discussion

Results obtained in the 0.5 kW$_{th}$ CLC unit can be useful to evaluate the potential of a material as oxygen carrier. In this sense, results obtained in this unit can be compared to results previously obtained with other oxygen carrier materials. In addition, an optimum design of a CLC unit would allow converting almost the entire char in the fuel reactor. Thus, the CO_2 capture in the process would be higher than values achieved in this work. These issues are now assessed.

4.1. Comparative evaluation between the use of Mn-ore and other Fe-based low cost materials

Several Fe-based oxygen carrier materials have been used previously in the 0.5 kW_{th} CLC unit burning bituminous coal, including ilmenite [28,38,39], an iron enriched sand fraction (Fe-ESF) from alumina production [29], and the highly reactive Tierga iron ore [30]. A proper selection of the results obtained with these materials can be used to perform a quantitative comparison regarding the CO_2 capture and oxygen demand achieved with different materials, which is useful to assess the potential of a material as oxygen carrier [40].

Regarding the oxygen demand, main influencing variables are the reactivity of oxygen carrier, and the solids circulation rate, [3]. Thus, a deep revision of available data for Fe-based materials was done in order to select operating conditions as similar as possible to those used in this work with the Mn-ore. The operating conditions are gathered in Table 4, and the total oxygen demand values of selected tests are shown in Figs. 9. Results with three different solids circulation rates were available for comparison purposes, corresponding to ϕ values for Mn-ore of 1.6, 2.5 and 4.5 aprox. However, the ϕ value for other materials was different because of the different oxygen transport capacity of each material; see Eq. (1).

Table 4. Operating conditions for selected tests to perform the comparative evaluation of the total oxygen demand shown in Figs. 9 between Mn-ore and other Fe-based materials used in the 0.5 kW_{th} CLC unit with bituminous coal.

	$\dot{m}_{OC}$ = 2.6 kg/s per MW_{th}		$\dot{m}_{OC}$ = 4.1 kg/s per MW_{th}		$\dot{m}_{OC}$ = 7.4kg/s per MW_{th}		Reference
	ϕ (-)	m^*_{FR} (kg/MW_{th})	ϕ (-)	m^*_{FR} (kg/MW_{th})	ϕ (-)	m^*_{FR} (kg/MW_{th})	
Mn-ore	1.6	1200-1300	2.5	1200-1300	4-5	1200-1500	This work
Ilmenite	1.1	1380	2.1	3400	-	-	[28,38,39]
Fe-ESF	-	-	1.3	2400-2800	1.9	2640	[29]
Fe-ore	-	-	1.1	1600-1800	-	-	[30]

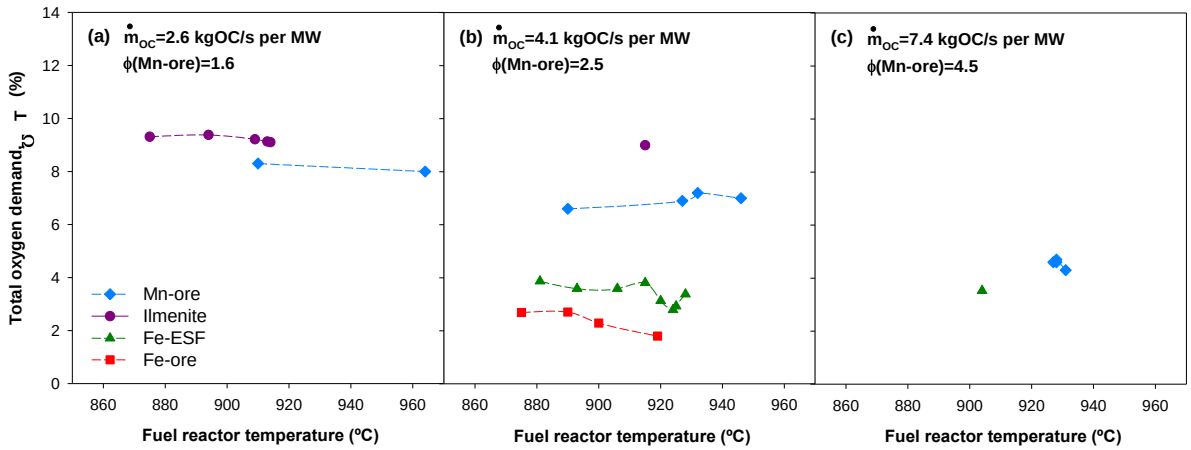

Fig. 9. Total oxygen demand values obtained in the 0.5 kW_{th} CLC unit with different oxygen carriers. Operating conditions corresponds to data shown in Table 4.

Complete combustion could not be achieved with any of the materials used based on Fe or Mn oxides. Uncomplete combustion is also a common finding in CLC units with a fuel reactor operating either in bubbling or circulating fluidization regime [3]. But it is highlighted in Fig. 9 that the total oxygen demand, Ω_T, is a function of the oxygen carrier reactivity. Thus, Tierga Fe-ore and Fe-ESF materials possess a high and similar reactivity with reacting gases such as H_2, CO or CH_4, while the reactivity of ilmenite was lower. Regarding the Mn-ore, the reactivity was found to be between those of ilmenite and Fe-ESF or Fe-ore [11], which agree with the tendency observed for Ω_T in Fig. 9. Thus, Ω_T values for Mn-ore were found to be between those of ilmenite and Fe-ESF or Fe-ore. However, it is intriguing that for the lower solids circulation rate Ω_T values for Mn-ore are close to those of ilmenite, i.e. relatively high Ω_T values, while they are closer to the values for Fe-ESF or Fe-ore as the solids circulation rate increases. Note that even in these cases, the solids inventory for Fe-ESF doubled that of the Mn-ore; see Table 4. Therefore, combustion efficiency achieved with the Mn-ore, are similar to those attained for the highly reactive Fe-ESF and Fe-ore materials, when a high solids circulation flow rate is chosen.

On the other hand, it is well known that the CO_2 capture efficiency is highly influenced by the coal rank, and the temperature and mean residence time of solids in the fuel reactor. In

general, the effect of the type of oxygen carrier was of lower relevance, which was deduced from results available with different Fe-based low cost materials [3,40]. But when results obtained with the Mn-ore are compared using the same coal, it can be deduced that this material allowed achieving higher CO_2 capture rates; see Fig. 10. This fact is directly related to the high char conversion rate observed with this Mn-ore at a lower scale [18], which is higher than that with Fe-based materials. This finding has been found to happen with other Mn-ore materials [17]. This behaviour has been related to the presence of certain amounts of K, Na or Ca in the Mn-ores which catalyse the char gasification [19]. Thus, a relatively high gasification rate was initially found for different manganese ores in a previous study, including the Mn-ore from Gabon used in the present study which present concentrations of 0.8 wt% K and 0.9 wt. Ca [18]. Then, the char gasification rate progressively decreased with the redox cycles. In most of the cases, the gasification rate was similar to that obtained using other Fe-based materials after 10 redox cycles, when most of K and Ca in the original particles were lost. However, the char gasification rate observed using the Mn-ore from Gabon stabilized in a value higher than that obtained with the Fe-based materials. This fact justifies the higher CO_2 capture rates achieved with the Mn-ore in the present work, but the ultimate reason for this behaviour needs further investigation.

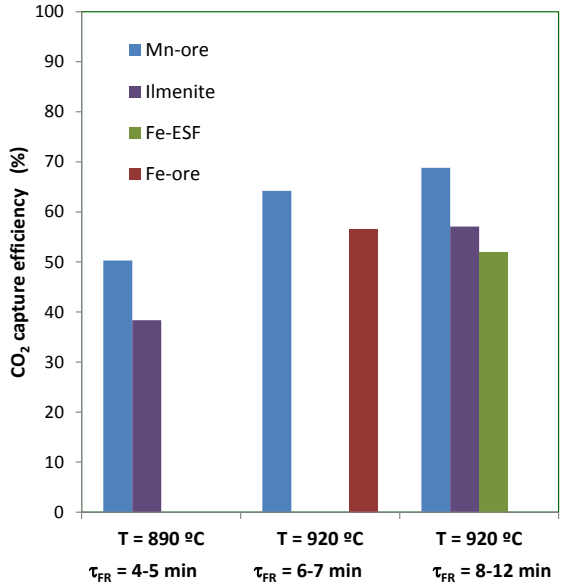

Fig. 10. CO_2 capture efficiency obtained in the 0.5 kW_{th} CLC unit with different oxygen carriers and similar values of temperature and mean residence time in the fuel reactor.

4.2. Extrapolation of experimental results for complete fuel conversion conditions

The 0.5 kW_{th} CLC unit, used in this work, has not dedicated devices to recover unconverted char exiting the fuel reactor, such as a carbon stripper for bypassed char to the air reactor or one cyclone to internally recirculate elutriated char. This configuration allows an easy evaluation of the coal conversion in the fuel reactor, more specifically the char conversion rate and its relation with the mean residence time of char in the fuel reactor; see Figs. 4 and 5. However, these results could be different if char conversion was improved in the fuel reactor by using such devices.

Considering that all elutriated char is internally recirculated to the fuel reactor (or no char elutriation happens), the resulting CO_2 capture efficiency, η_{CC}^{*}, can be easily calculated by [30]:

$$\eta_{CC}^{*} = 1 - \frac{x_{C,fix}}{x_C} \cdot (1 - X_{char,FR}) \tag{11}$$

In this way, the estimated value for the CO_2 capture at the maximum temperature achieved in the CLC unit, see Fig. 5(a), is η_{CC}^{*} = 82.5 %. In order to increase the CO_2 capture efficiency in the CLC process, a carbon separation unit must be arranged in the unit; see Fig. 1. The efficiency of this device separating unconverted char from the oxygen carrier stream, η_{CSS}, would determine the actual CO_2 capture efficiency of the system assuming the fuel reactor being a fluidized bed [30].

$$\eta_{CC}^{*} = 1 - \frac{x_{C,fix}}{x_C} \cdot \frac{\dot{m}_{OC}^{*} \cdot (1 - \eta_{CSS})}{(-r_C) \cdot m_{FR}^{*} + \dot{m}_{OC}^{*} \cdot (1 - \eta_{CSS})} \tag{12}$$

In a previous work [32], suitable design parameters for the scale-up of CLC with coal were determined to be a specific solids inventory of 750 kg/MW_{th} as well as a specific circulation

rate of $\dot{m}^{*}_{OC}$ = 5 kg/s per MW_{th} , corresponding to an oxygen carrier to fuel ratio of ϕ = 3, for the Mn-ore.

Considering these values as optimum operation conditions, the CO_2 capture efficiency can be estimated as a function of the efficiency of the carbon separation system, η_{CCS} using the char gasification rate calculated for test T22 at 964 ºC ($-r_C$) = $8 \cdot 10^{-3}$ s^{-1}; see Fig. 11. Also, the CO_2 capture at a fuel reactor temperature of 1000 ºC was also estimated using in this case, Eq. (10) to calculate a value of ($-r_C$) = $1.6 \cdot 10^{-2}$ s^{-1}. Note that a temperature about 1000 ºC is advised in CLC with coal in order to improve the char conversion [36,41].

As it can be seen, the higher temperature improved the CO_2 capture rate. Considering a threshold value of η_{CC} = 95 %, the required efficiency of a carbon separation system would be 92.2 % at 964 ºC and 84.2 % at 1000 ºC. These values can be reached in operational pilot plants [35,42]. Considering the promising results obtained with the Mn-ore at the 0.5 kW_{th} scale, this material is a good candidate to evaluate it in a CLC unit with a carbon stripper in the future.

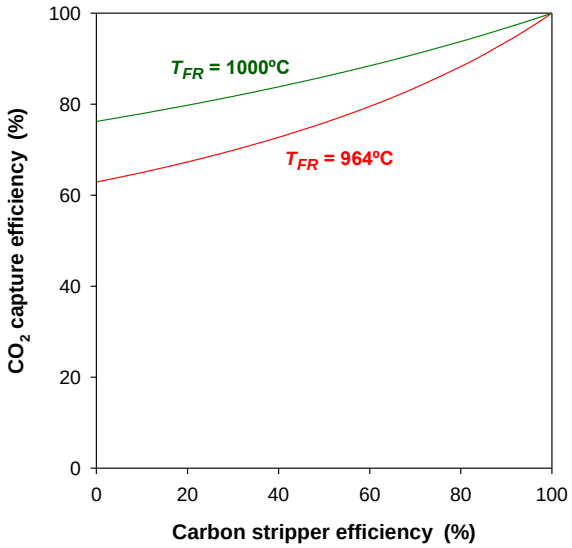

Fig. 11. Estimated CO_2 capture efficiency, η^{*}_{CC} , as a function of the efficiency of the carbon separation system, η_{CCS}, at T_{FR} = 964 ºC and 1000 ºC using; m^{*}_{FR} = 750 kg/MW_{th}; ϕ = 3.

To analyse the combustion degree achieved by the oxygen carrier, a deeper analysis of the combustion efficiency obtained in the unit is presented below. The method developed by

Adánez et al. [3] is used to estimate the combustion efficiency of the volatile matter, $\eta_{comb,v}$, and the gasification products, $\eta_{comb,g}$ which can be calculated by means of the following expression:

$$A = (1-\eta_{comb,v}) + (1-\eta_{comb,g}) \cdot B \tag{13}$$

$$A = \frac{\Omega_{char}(1-x_{char,FR})}{\Omega_{vol}\left[\frac{1}{\Omega_T} - \frac{1}{\Omega_{FR}}\right]}$$

$$B = \frac{\Omega_{char}}{\Omega_{vol}} x_{char,FR}$$

$x_{char,FR}$ being the carbon fraction in char being converted only in the fuel reactor calculated as:

$$x_{char,FR} = X_{char} X_{char,FR} = 1-(1-\eta_{CC} X_{sf})\left(\frac{x_C}{x_{C,fix}}\right) \tag{14}$$

A and *B* parameters must be calculated for conditions which the mean reactivity of the oxygen carrier particles was approximately constant, and considering tests with different values of $x_{char,FR}$. Thus, experiments at similar fuel reactor temperature for ϕ > 3 where selected for this calculation; see tests T3-T11. From the B vs. A plot in Fig. 12, values of $\eta_{comb,v}$ = 88.5 % and $\eta_{comb,g}$ = 95.1 % can be deduced from the y-intercept and the slope of the linear regression of data; see Eq. (13). The high combustion degree of gasification products agrees to those expected from the analysis of the effect of the solids inventory on the total oxygen demand; see discussion of Fig. 7.

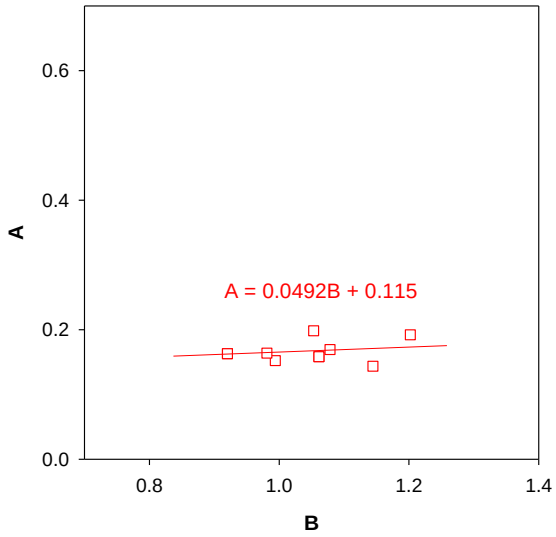

Fig. 12. Determination of A and B parameters of Eq. (13) to evaluate the combustion efficiency of the volatile matter, $\eta_{comb,v}$, and products of char gasification, $\eta_{comb,g}$, following method by Adánez et al. [3].

Once $\eta_{comb,v}$ and $\eta_{comb,g}$ are known, the oxygen demand at complete conversion of the fuel in the fuel reactor can be estimated using Eq. (15) for $x_{char,FR}$ = 1. In such case, a value of $\Omega_{T,full}$ = 6.8 % is calculated for the Mn-ore. Note that $\Omega_{T,full}$ estimates the oxygen demand which would be obtained if all the char was converted in the fuel reactor, i.e. neither unconverted char was bypassed to the air reactor nor char was elutriated from the fuel reactor. Thus, $\Omega_{T,full}$ can be used to compare the performance of the combustion of a solid fuel with different oxygen carrier materials or in different CLC units [3]. Thus, $\Omega_{T,full}$ is a useful parameter to compare the results obtained with different oxygen carrier materials in a CLC unit when the fraction of char converted in the fuel reactor are different.

$$\Omega_T = \frac{(1-\eta_{comb,v})\cdot\Omega_{vol} + (1-\eta_{comb,g})\cdot\Omega_{char}\,x_{char,FR}}{\Omega_{coal}} \quad (15)$$

Experiments carried out with ilmenite, Fe-ore or Fe-ESF were characterized by a lower char conversion in the fuel reactor, resulting in lower CO_2 capture rates (see Fig. 10) which can affect to the oxygen demand. To eliminate the effect of the different values of CO_2 capture, $\Omega_{T,full}$ obtained with the Mn-ore ($\Omega_{T,full}$ = 6.8 %) can be compared with those calculated for

ilmenite ($\Omega_{T,full}$=12.6 %) or Fe-ESF ($\Omega_{T,full}$=8.4 %) in [3]. Thus, $\Omega_{T,full}$ for the Mn-ore is the lowest determined with other low cost materials. This comparison realizes the promising good behaviour of this Mn ore regarding both oxygen demand and CO_2 capture efficiency expected in CLC scale-up process

5. Conclusions

Coal combustion tests performed in the 0.5 kW_{th} CLC continuous unit allowed an assessment of the use of a Mn-ore from Gabon as oxygen carrier. The effect of several operating conditions on the CO_2 capture and combustion efficiencies was assessed. Variations in the operating conditions increasing the mean residence time of solids in the fuel reactor -i.e. increase of the solids inventory or decrease of the solids circulation- resulted in an increase of the CO_2 capture due to the higher char conversion in the fuel reactor. The same tendency was observed with an increase of the fuel reactor temperature, and a direct relation between the char gasification rate and the reacting temperature was determined. Although relatively low CO_2 capture values were reached in the 0.5 kW_{th} CLC unit, the CO_2 capture would be easily increased above 95% by using a carbon separation system, e.g. a carbon striper, to separate unburned char from the oxygen carrier.

Uncomplete combustion of coal was found in the fuel reactor. Minimum values of the total oxygen demand in the Ω_T = 4-5 % interval was found. The combustion efficiency was mainly affected by the solids circulation rate, being the temperature and the solids inventory in the fuel reactor of minor relevance in the studied interval. It was determined that most of unconverted gases from the fuel reactor come from volatile matter.

A certain dilution of steam with recirculated CO_2, up to 50 % aprox., would be allowed for the fluidizing gas of the fuel reactor. At this condition, no dramatic decrease of the CO_2 capture was found, being its effect on the combustion efficiency of minor relevance.

Results obtained in this work show that the Mn-ore is a feasible oxygen carrier for CLC with solid fuels, and it is a good alternative to low-cost Fe-based materials. Similar values of total oxygen demand to those achieved by highly reactive iron materials, such as Tierga iron ore

or iron enriched sand fraction (Fe-ESF) can be achieved with suitable oxygen carrier circulation rates. In addition, it is highly relevant the high values obtained for the CO_2 capture efficiency, which is related to the higher char gasification rate in the presence of the Mn-ore. The ultimate reason for that must be further investigated in the future.

Moreover, the estimated total oxygen demand at full fuel conversion ($\Omega_{T,full}$ = 6.8 %) was the lowest determined with other low cost materials used in the same facility. This result highlight the promising performance of this Mn-ore regarding both oxygen demand and carbon capture efficiency expected in the next scale-up of the CLC process.

Acknowledgements

This work was partially supported by the Ministry of Economy, Industry and Competitiveness via ENE2014-56857-R, ENE2016-77982-R and CSIC-2017-80E035 projects, and the European Regional Development Fund (ERDF). J.A. Bueno thanks for the FPI Fellowship. T. Mendiara thanks for the ‘‘Ramón y Cajal’’ post-doctoral contract. The authors also thank Hidro Nitro Española S.A. for providing Mn material.

Nomenclature

E_a	activation energy (J/mol)
F_i	molar flow of the compound *i* (mol/s)
$k_{0,app}$	pre-exponential factor of the apparent kinetic constant (s^{-1})
M_i	molecular/atomic weight of species *i* (kg/mol)
m_{FR}	mass of solids in the fuel reactor (kg)
m^*_{FR}	specific solids inventory in the fuel reactor (kg/MW)
$\dot{m}_{coal}$	mass flow of coal (kg/s)
$\dot{m}_{OC}$	mass flow of recirculated oxygen carier (kg/s)
R_g	ideal gas constant (=8.314 J mol^{-1} K^{-1})
R_{OC}	oxygen transport capacity of the oxygen carrier (-)
$(-r_C)$	char gasification rate (s^{-1})
T_{FR}	fuel reactor temperature (K)
X_{char}	conversion of char in the whole CLC unit (-)
$X_{char,FR}$	conversion of char in the fuel reactor (-)
X_{sf}	conversion of solid fuel (-)
x_C	fraction of carbon in solid fuel (-)
$x_{C,fix}$	fraction of fixed carbon in solid fuel (-)
$x_{char,FR}$	fraction of carbon in char converted in the fuel reactor (-)

Greek symbols

ϕ	oxygen carrier to fuel ratio (-)
η_{CC}	CO_2 capture efficiency (-)
η^*_{CC}	estimated CO_2 capture efficiency (-)
η_{CSS}	efficiency of the carbon separation system (-)
$\eta_{comb,FR}$	combustion efficiency in the fuel reactor (-)
$\eta_{comb,g}$	combustion efficiency of the char gasification products (-)
$\eta_{comb,v}$	combustion efficiency of the volatiles (-)
τ_{FR}	mean residence time of solids (s)
Ω_{char}	oxygen demand of the char (kg O/kg solid fuel)
Ω_{FR}	oxygen demand in the fuel reactor (-)
Ω_{coal}	oxygen demand of the coal (kg O/kg solid fuel)
Ω_T	total oxygen demand (-)
$\Omega_{T,full}$	total oxygen demand for complete fuel conversion in the fuel reactor (-)
Ω_{vol}	oxygen demand of the volatiles (kg O/kg solid fuel)

Subscripts:

C,elut	elutriated carbon
inFR	inlet to fuel reactor
outAR	outlet from air reactor
outFR	outlet from fuel reactor
vol	volatile matter

References

[1] E.S. Rubin, H. Mantripragada, A. Marks, P. Versteeg, J. Kitchin. The outlook for improved carbon capture technology. Prog. Energy Comb. Sci. 38 (2012) 630-671.

[2] J. Adánez, A. Abad, F. García-Labiano, P. Gayán, L.F. de Diego. Progress in Chemical-Looping Combustion and Reforming Technologies. A review. Prog. Energy Combust. Sci. 38 (2012) 215-282.

[3] J. Adánez, A. Abad, T. Mendiara, P. Gayán, L.F. de Diego, F. García-Labiano. Review and assessment of experimental results from chemical looping combustion units burning solid fuels. Prog. Energy Combust. Sci. 65 (2018) 6-66.

[4] A. Lyngfelt. Chemical-looping combustion of solid fuels - Status of development. Applied Energy 113 (2014) 1869-1873.

[5] P. Gayán, A. Abad, L.F. de Diego, F. García-Labiano, J. Adánez. Assessment of technological solutions for improving chemical looping combustion of solid fuels with CO_2 capture. Chem. Eng. J. 233 (2013) 56-69.

[6] F. García-Labiano, L.F. de Diego, P. Gayán, A. Abad, J. Adánez. Fuel reactor modelling in chemical-looping combustion of coal: 2-simulation and optimization. Chem. Eng. Sci. 87 (2013) 173-182.

[7] B. Wang, H. Zhao, Y. Zheng, Z. Liu, R. Yan, C. Zheng. Chemical looping combustion of a Chinese anthracite with Fe_2O_3-based and CuO-based oxygen carriers. Fuel Process. Technol. 96 (2012) 104-115.

[8] T. Mendiara, P. Gayán, A. Abad, L.F. de Diego, F. García-Labiano, J. Adánez. Performance of a bauxite waste as oxygen-carrier for chemical-looping combustion using coal as fuel. Fuel Process. Technol. 109 (2013) 57-69.

[9] H. Leion, T. Mattisson, A. Lyngfelt. Use of Ores and Industrial Products As Oxygen Carriers in Chemical-Looping Combustion. Energy Fuels 23 (2009) 2307-2315.

[10] A. Fossdal, E. Bakken, B.A. Oye, C. Schoning, I. Kaus, T. Mokkelbost, Y. Larring. Study of inexpensive oxygen carriers for chemical looping combustion. Int. J. Greenhouse Gas Control 5 (2011) 483-488.

[11] D. Mei, T. Mendiara, A. Abad, L.F. de Diego, F. Garcia-Labiano, P. Gayan, J. Adanez, H. Zhao. Evaluation of Manganese minerals for Chemical Looping Combustion. Energy Fuels 29 (2015) 6605-6615.

[12] F.J. Velasco-Sarria, C.R. Forero, I. Adánez-Rubio, A. Abad, J. Adánez. Assessment of low-cost oxygen carrier in South-western Colombia, and its use in the in-situ gasification chemical looping combustion technology. Fuel (2018).

[13] M. Arjmand, H. Leion, T. Mattisson, A. Lyngfelt. Investigation of different manganese ores as oxygen carriers in chemical-looping combustion (CLC) for solid fuels. Appl. Energ. 113 (2014) 1883-1894.

[14] S. Sundqvist, M. Arjmand, T. Mattisson, M. Rydén, A. Lyngfelt. Screening of different manganese ores for chemical-loopingcombustion (CLC) and chemical-looping with oxygen uncoupling(CLOU). Int. J. Greenhouse Gas Control 43 (2015) 179-188.

[15] Y. Larring, M. Pishahang, M.F. Sunding, K. Tsakalakis. Fe–Mn based minerals with remarkable redox characteristics for chemical looping combustion. Fuel 159 (2015) 169-178.

[16] P. Frohn, M. Arjmand, G. Azimi, H. Leion, T. Mattisson, A. Lyngfelt. On the High-Gasification Rate of Brazilian Manganese Ore in Chemical-Looping Combustion (CLC) for Solid Fuels. AIChE J. 59 (2013) 4346-4354.

[17] M. Arjmand, H. Leion, A. Lyngfelt, T. Mattisson. Use of manganese ore in chemical-looping combustion (CLC) - Effect on steam gasification. Int. J. Greenhouse Gas Control 8 (2012) 56-60.

[18] D. Mei, T. Mendiara, A. Abad, L.F. de Diego, F. Garcia-Labiano, P. Gayan, J. Adanez, H. Zhao. Manganese minerals as oxygen carriers for chemical looping combustion of coal. Ind. Eng. Chem. Res. 55 (2016) 6539-6546.

[19] M. Keller, H. Leion, T. Mattisson. Mechanism of Solid Fuel Conversion by Chemical-Looping Combustion (CLC) using Manganese Ore: Catalytic Gasification by Potasium Compounds. Energy Technology 1 (2013) 273-282.

[20] Z. Yu, C. Li, X. Jing, Q. Zhang, Z. Wang, Y. Fang, J. Huang. Catalytic chemical looping combustion of carbon with an iron-based oxygen carrier modified by K_2CO_3: Catalytic mechanism and multicycle tests. Fuel Process. Technol. 135 (2015) 119-124.

[21] C. Linderholm, A. Lyngfelt, A. Cuadrat, E. Jerndal. Chemical-looping combustion of solid fuels - Operation in a 10 kW unit with two fuels, above-bed and in-bed fuel feed and two oxygen carriers, manganese ore and ilmenite. Fuel 102 (2012) 808-822.

[22] C. Linderholm, M. Schmitz, P. Knutsson, A. Lyngfelt. Chemical-looping combustion in a 100-kW unit using a mixture of ilmenite and manganese ore as oxygen carrier. Fuel 166 (2016) 533-542.

[23] M. Schmitz, C. Linderholm, P. Hallberg, S. Sundqvist, A. Lyngfelt. Chemical-Looping Combustion of Solid Fuels Using Manganese Ores as Oxygen Carriers. Energy Fuels 30 (2016) 1204-1216.

[24] C. Linderholm, M. Schmitz, M. Biermann, M. Hanning, A. Lyngfelt. Chemical-looping combustion of solid fuel in a 100 kW_{th} unit using sintered manganese ore as oxygen carrier. Int. J. Greenhouse Gas Control 65 (2017) 170-181.

[25] T. Pikkarainen, I. Hiltunen. Chemical Looping Combustion of solid biomass – Performance of ilmenite and braunite as oxygen carrier materials. Proc. from the 25th European Biomass Conference and Exhibition, Stockholm, Sweden (2017).

[26] T. Berdugo Vilches, F. Lind, M. Rydén, H. Thunman. Experience of more than 1000 h of operation with oxygen carriers and solid biomass at large scale. Applied Energy 190 (2017) 1174-1183.

[27] A. Cabello, P. Gayán, F. García-Labiano, L.F. de Diego, A. Abad, J. Adánez. On the attrition evaluation of oxygen carriers in Chemical Looping Combustion. Fuel Process. Technol. 148 (2016) 188-197.

[28] A. Cuadrat, A. Abad, F. García-Labiano, P. Gayán, L.F. de Diego, J. Adánez. The use of ilmenite as oxygen-carrier in a 500 W_{th} Chemical-Looping Coal Combustion unit. Int. J. Greenhouse Gas Control 5 (2011) 1630-1642.

[29] T. Mendiara, L.F. de Diego, F. García-Labiano, P. Gayán, A. Abad, J. Adánez. Behaviour of a bauxite waste material as oxygen carrier in a 500 W_{th} CLC unit with coal. Int. J. Greenhouse Gas Control 17 (2013) 170-182.

[30] T. Mendiara, L.F. de Diego, F. García-Labiano, P. Gayán, A. Abad, J. Adánez. On the use of a highly reactive iron ore in Chemical Looping Combustion of different coals. Fuel 126 (2014) 239-249.

[31] T. Mendiara, A. Abad, L.F. de Diego, F. García-Labiano, P. Gayán, J. Adánez. Use of an Fe-Based Residue from Alumina Production as an Oxygen Carrier in Chemical-Looping Combustion. Energy Fuels 26 (2012) 1420-1431.

[32][39] A. Abad, J. Adánez, P. Gayán, L.F. de Diego, F. García-Labiano, G. Sprachmann. Conceptual design of a 100 MW_{th} CLC unit for solid fuel combustion. Applied Energy 157 (2015) 462-474.

[33] P. Simell, P. Stahlberg, E. Kurkela, J. Albretch, S. Deutch, K. Sjostrom. Provisional protocol for the sampling and analysis of tar and particulates in the gas from large-scale biomass gasifiers. Version 1998. Biomass and Bioenergy 18 (2000) 19-38.

[34][33][32] T. Mattisson, A. Lyngfelt, H. Leion. Chemical-looping with oxygen uncoupling for combustion of solid fuels. Int. J. Greenhouse Gas Control 3 (2009) 11-19.

[35][34][33] A. Abad, J. Adánez, L.F. de Diego, P. Gayán, F. García-Labiano, A. Lyngfelt. Fuel reactor model validation: Assessment of the key parameters affecting the chemical-looping combustion of coal. Int. J. Greenhouse Gas Control 19 (2013) 541-551.

[36][35][34] R. Pérez-Vega, A. Abad, F. García-Labiano, P. Gayán, L.F. de Diego, J. Adánez. Coal combustion in a 50 kW_{th} Chemical Looping Combustion unit: Seeking operating conditions to maximize CO_2 capture and combustion efficiency. Int. J. Greenhouse Gas Control 50 (2016) 80-92.

[37][36][35] A. Abad, J. Adánez, F. García-Labiano, L.F. de Diego, P. Gayán, J. Celaya. Mapping of the range of operational conditions for Cu-, Fe-, and Ni-based oxygen carriers in chemical-looping combustion. Chem. Eng. Sci. 62 (2007) 533-549.

[38][37][36] A. Cuadrat, A. Abad, F. García-Labiano, P. Gayán, L.F. de Diego, J. Adánez. Effect of operating conditions in Chemical-Looping Combustion of coal in a 500 W_{th} unit. Int. J. Greenhouse Gas Control 6 (2012a) 153-163.

[39][38][37] A. Cuadrat, A. Abad, F. García-Labiano, P. Gayán, L.F. de Diego, J. Adánez. Relevance of the coal rank on the performance of the in situ gasification chemical-looping combustion. Chem. Eng. J. 195-196 (2012b) 91-102.

[40][39][38] A. Abad, T. Mendiara, P. Gayán, F. García-Labiano, L.F. de Diego, J.A. Bueno, R. Pérez-Vega, J. Adánez. Comparative Evaluation of the Performance of Coal Combustion in 0.5 and 50 kW_{th} Chemical Looping Combustion units with ilmenite, redmud or iron ore as oxygen carrier. Energy Procedia 114 (2017) 285-301.

[41][40] N. Berguerand, A. Lyngfelt. Chemical-Looping Combustion of Petroleum Coke Using Ilmenite in a 10 kW_{th} Unit – High-Temperature Operation. Energy Fuels 23 (2009) 5257-5268.

[42][41] M. Kramp, A. Thon, E.-U. Hartge, S. Heinrich, J. Werther. Carbon stripping – a critical process step in chemical looping combustion of solid fuels. Chem. Eng. Technol. 35 (2012) 497-507.